American Journal of Chemistry 2018, 8(3): 72-83
DOI: 10.5923/j.chemistry.20180803.03

Synthesis and Characterization of Novel Glassy Titanium-, Zirconium Tellurates-Fibrous Cerium Phosphate/ Polyaniline, Polyindole, Polypyrrole, Polyaniline-co-Polyindole, Polyaniline-co-Polypyrrole Nanocomposite Membranes

S. K. Shakshooki[1,*], M. B. Hassan[2], Ibtihal M. Abdullah[2]

[1]Department of Chemistry, Faculty of Science, University of Tripoli, Tripoli, Libya
[2]Department of Chemistry, Faculty of Science, University of Sebha, Sebha, Libya

Abstract Glassy titanium tellurate, $TiO(HTeO_4)_2.3.99H_2O$ (TiTe), Glassy zirconium tellurate, $ZrO(HTeO_4)_2.\ 3.35H_2O$ (ZrTe) and nano fibrous cerium phosphate, $Ce(HPO_4)_2.2.9H_2O$(nCeP_f), were prepared and characterized by chemical, XRD, TGA, FT-IR and SEM. Mixing slurry aqueous solutions of TiTe-, ZrTe with slurry aqueous solution of nCeP_f (in 25:75 wt/wt% mixing ratios), respectively, lead to formation of novel titanium tellurate/ fibrous cerium phosphate, zirconium tellurate/fibrous cerium phosphate nanocomposite membranes, $[TiO(HTeO_4)_2]_{0.25}[Ce(HPO_4)_2]_{0.75}\ .1.75\ H_2O$, (TiTe-n$CeP_f$), and $[ZrO(HTeO_4)_2]_{0.25}\ [Ce(HPO_4)_2]_{0.75}.2.11H_2O$(ZrTe-n$CeP_f$), respectively. They were characterized by XRD TGA and FT-IR. Their /polyaniline-, polyindole-, polypyrrole-, polyaniline–co-polyindole-, polyaniline-co-polypyrrole nanocomposite membranes were prepared via in-situ chemical oxidation of the monomers aniline, indole, pyrrole and (1:1moler ratio) of co-monomers aniline-indole, aniline- pyrrole, respectively, that was promoted by the reduction of Ce(iv) ions present in the inorganic matrix of (TiTe-nCeP_f and ZrTe-nCeP_f) nanocomposite membranes, respectively. A possible explanation is nCeP_f present on the surface of the fibrous cerium phosphate membrane is attacked by the monomers, and the co-monomers, respectively, converted to cerium (III) orthophosphate ($CePO_4$). The resultant materials were characterized by elemental (C,H,N) analysis, FT-IR, and scanning electron microscopy(SEM). From elemental (C,H,N) analysis the amount of organic materials present in (TiTe-nCeP_f)/polyaniline-, polyindole-, polypyrrole composites were (14.88, 11.87, 10.73 % in wt), respectively. The amount of organic materials present in (ZrTe-nCeP_f)/Polyaniline-, polyindole-, polypyrrole composites (22.8, 5.52, 7.58 % in Wt), respectively. Organic material present in composite (TiTe-nCeP_f)/ polyaniline-co-polyindole were (Pani 9.92, PIn 10.43 % in wt). Amount of organic material in composite (TiTe-nCeP_f)/ polyaniline-co-polypyrrole were (Pani 9.55, PPy 5.1 % in wt). Amount of organic materials in composite (ZrTe-nCeP_f)/ polyaniline-co-polyindole were (Pani 7.15, PIn 10.76 % in wt), for composite (ZrTe-nCeP_f)/ polyaniline-co-polypyrrole (Pani 16.24, PPy 4.68 % in wt). These composites can be considered as novel conducting inorganic-organic composites, ion exchangers, solid acid catalysts and sensors.

Keywords Glassy titanium-, Zirconium tellurates -cerium phosphate nanocomposites, Polyaniline, Poly indole, Polypyrrole, Copolymers nanocomposites

1. Introduction

Conducting polymers are a novel class of synthetic metals that combine the chemical, electrochemical and mechanical properties of polymers with the electronic properties of metals and semiconductor, generated tremendous interest due to their potential applications in various fields such as rechargeable batteries, electrochromic display devices, separation membranes, sensors and anticorrosive coatings on metals [1-11].

Conducting polymers containing nitrogen atoms such as polyaniline, polypyrrole, and polyindole and their substituted derivatives, belonging to the fused-ring family, have received increasing attention in various fields due to their unique physical, electrical and chemical properties

* Corresponding author:
shakshooki2002@yahoo.com (S. K. Shakshooki)
Published online at http://journal.sapub.org/chemistry

[1-10]. These materials have an important influence on electrochromic device, sensors, catalysis, anticorrosion. Their electrical and electrochemical properties, owns advantages fairly good thermal stability show great promise for commercial applications [12-17].

Among conductive polymers, polyaniline (Pani) has attracted considerable attention, widely studied, because of its ease of preparation, low cost of monomer, good environmental stability, good conductivity control through doping as well as a good control of oxidation level. All these properties give Pani the potential for wide applications [17-21]. It can effectively be used as opto-electronic sensors [22-25], conductive paints and adhesive [26-28]. Pani has also good power and energy density, so it has been analysed for the development of new super capacitor materials [29-32].

Polypyrrole (PPy) also has attracted considerable attention, widely considered conducting polymer and the most used polymer in commercial application. It shows good long term stability of its electric conductivity [8, 9, 11, 15, 33-37].

Polyindole is an electro active polymer, owns advantages especially fairly good thermal stability [38, 39]. Some studies shows polyindole has similar properties like polyaniline, based on their high conductance and good environmental stability [40-44].

Inorganic layered nanomaterials are receiving great attention because of their size, structure, and possible biochemical applications [45, 46], that have been proven to be good carriers for organic polar molecules. Examples of these are zirconium phosphates, $Zr(HPO_4)_2{\cdot}nH_2O$(ZrP), (where n=1-5) which are inorganic cation exchange materials with high thermal stability, solid-state ion conductivity, resistance to ionizing radiation, and which are known as hosts capable of incorporating different types and sizes of guest molecules [46].

Crystalline cerium phosphates have been studied for a long time as ion exchangers, their structures remains unknown until recently [47-49]. The reason is that, the composition, the structure and the degree of crystallinity of their precipitates results from reaction of solutions containing a Ce(iv) salt which is mixed with a solution of phosphoric acid of [(PO_4)/Ce(iv) ratio], strongly depend on the experimental conditions such as rate and order of mixing of the solutions, stirring, temperature and digestion time, this also implemented on fibrous cerium phosphate [50]. To date, most of the work on fibrous cerium phosphate was carried out on its ion exchange [51], intercalation [52] and electrical conductance properties [53].

Organic-inorganic nanocomposite membranes have gained great attention recently [54, 55]. The composite material may combine the advantage of each material, for instance, flexibility, processability of polymers and the selectivity and thermal stability of the inorganic filler [54-59].

In our laboratory, we are carrying systematic investigations on novel tetravalent metal phosphates and tetravalent metal tellurates /organic conducting polymers nanocomposite membranes. Fibrous cerium phosphate/ polybenzimidazole-, polyindole-, polyaniline nanocomposite membranes were reported [60-62].

The present study describes the preparation and characterization of novel conductive polymers nanocomposite membranes of fibrous cerium phosphate Ti-, Zr tellurates / polyaniline-, polyindole-, polypyrrole and their copolymers.

2. Materials and Methods

2.1. Chemicals

$Ce(SO_4)_2.4H_2O$ of (Merck), $ZrOCl_2.8H_2O$, $TiCl_4$, of (BDH), telluric acid $(TeH_2O_4).2H_2O$ of (Fluka), HF (40%) of Reidel-Dehaen, aniline (99.5%) of (Mindex UK) indole of (PARK), pyrrole of (Aldrich), Other reagents used were of analytical grade.

2.2. Instruments Used for Characterization

X-Ray powder diffractometry Siemens D-500, using Ni-filtered CuKα (λ=1.54056Å), TG/DTA SIIExtra6000, CHN-Elemental analyzer, Vario Elemental-German, Fourier Transform IR spectrometer, model FT/IR-6100, Scanning electron microscopy (SEM) Jeol SMJ Sm 5610 LV. and pH Meter WGW 52.

2.3. Preparation of Nanofibrous Cerium Phosphate Membrane, $Ce(HPO_4)_2.2.9H_2O$ ($nCeP_f$)

Nanofibrous cerium phosphate membrane was prepared from adding 250 ml of 0.05M $CeSO_4.4H_2O$ in 0.5 M H_2SO_4 solution, drop wise, to 250 ml of 6 M H_3PO_4 at ~ 80°C with stirring. After complete addition the resultant material left to digest at that temperature for 4h. To that 750 ml of hot distilled water, (~60°C), was added with stirring for 1h. The resultant slurry aqueous solution of nanofibrous cerium phosphate was kept. The sheet form of nanofibrous cerium phosphate membrane can be obtained by filtration of the resultant slurry aqueous solution on Buchner funnel.

2.4. Preparation of Glassy Titanium Tellurate

3.5g telluric acid was dissolved in 50 ml distilled water at 55 °C. To that 25ml of 0.5M $TiCl_4$ in 4M HCl were added with stirring, the stirring was continued for one hour. After that 5M NaOH solution was added gradually with stirring, up to pH about 2.5. The resultant gel was left to digest in mother liquor for 48h, then filtered, washed with distilled water up to pH=3, and dried at 60°C, then water cracked. Glassy titanium tellurate was obtained on filtration, left to dry in air. Found to be $TiO(HTeO_4)_2.3.99H_2O$, designated as TiTe.

2.5. Preparation of Glassy Zirconium Tellurate

6g telluric acid was dissolved in 50 ml distilled water at 55°C. To that an aqueous solution of 4g $ZrOCl_2.8H_2O$ in 25ml H_2O was added with stirring, the stirring was continued for three hours. The resultant gel was left to digest in mother

liquor for 48h, then filtered, washed with distilled water up to pH=3, and dried at 60°C, then water cracked. Glassy zirconium tellurate was obtained on filtration, left to dry in air. Found to be $ZrO(HTeO_4)_2.\ 3.35H_2O$, designated as ZrTe.

2.6. Preparation of Glassy Titanium Tellurate -fibrous Cerium Phosphate Nanocomposite Membrane (TiTe-nCeP$_f$)

525ml of slurry cerium phosphate (2.1g nCeP$_f$) were added to 0.7g of glassy titanium tellurate at 45°C with stirring for 3hours. The mixture were left at room temperature for 24 hours. The contents were stirred for an hour, filtered on Buchner funnel then washed with distilled water. The resultant sheet left to dry in air.

2.7. Preparation of Glassy Zirconium Tellurate -fibrous Cerium Phosphate Nanocomposite Membrane (ZrTe-nCeP$_f$)

525ml of slurry cerium phosphate (2.1g nCeP$_f$) were added to 0.7g of glassy zirconium tellurate at 45°C with stirring for 3hours. The resultant mixture left at room temperature for 24 hours. The contents were stirred for an hour, filtered on Buchner funnel, washed with distilled water. The resultant sheet left to dry in air.

2.8. (TiTe-nCeP$_f$) Nanocomposite Membrane Self Support Polymerization of Aniline, Indole, and Pyrrole

2.8.1. Polymerization of Aniline

0.2g of TiTe-nCeP$_f$ sheet was immersed in 10ml of 4% aniline in ethanol, left at room temperature for 48h. The impregnated sheet was removed, washed with distilled water and ethanol and left to dry in air. The colour of the resultant product was dark green.

2.8.2. Polymerization of Indole

0.2g of TiTe-nCeP$_f$ sheet was immersed in 12 ml of 4% indole in ethanol, left at room temperature for 48h. The impregnated sheet was removed, washed with distilled water and ethanol and left to dry in air. The colour of the resultant product was brown.

2.8.3. Polymerization of Pyrrole

0.2g of TiTe-nCeP$_f$ sheet was immersed in 7.5 ml of 4% pyrrole in ethanol, left at room temperature for 48h. The impregnated sheet was removed, washed with distilled water and ethanol and left to dry in air. The colour of the resultant product was black.

2.9. (ZrTe-nCeP$_f$) Nanocomposite Membrane Self Support Polymerization of Aniline, Indole, and Pyrrole

2.9.1. Preparation of (ZrTe-nCeP$_f$) / Polyaniline, Polyindole and Polypyrrole Composites, Respectively

Implementation similar experimental parameters showed above, polymerization of aniline, indole and pyrrole was carried out by immersing 0.2g of ZrTe-nCeP$_f$ nanocomposite sheet into (4% solutions of 10ml aniline, 12ml indole and 7.5ml pyrrole), respectively. The colors of the resultant products were, dark green, brown, and black, respectively.

2.10. (TiTe-nCeP$_f$) Nanocomposite Membrane Self Support Polymerization of Co-monomers Aniline-indole, and Aniline-pyrrole

2.10.1. Preparation of (TiTe-nCeP$_f$) / Polyaniline-co-polyindole Composite

0.270g of TiTe-nCeP$_f$ sheet was immersed in a mixture of 5ml of 4% aniline and 6 ml 4% indole in ethanol, left at room temperature for 48h. The impregnated sheet was removed, washed with distilled water and ethanol and left to dry in air. The colour of the resultant product was green.

2.10.2. Preparation of (TiTe-nCeP$_f$) / Polyaniline-co-polypyrrole Composite

0.275g of TiTe-nCeP$_f$ sheet was immersed in a mixture of 5ml of 4% aniline and 3.75 ml 4% pyrrole in ethanol, left at room temperature for 48h. The impregnated sheet was removed, washed with distilled water and ethanol and left to dry in air. The colour of the resultant product was blackish-green.

2.10.3. Preparation of (ZrTe-nCeP$_f$) / Polyaniline-co-polyindole Composite

0.30g of ZrTe-nCeP$_f$ sheet was immersed in a mixture of 5ml of 4% aniline and 6 ml 4% indole in ethanol, left at room temperature for 48h. The impregnated sheet was removed, washed with distilled water and ethanol and left to dry in air. The colour of the resultant product was green.

2.10.4. Preparation of (ZrTe-nCeP$_f$) / Polyaniline-co-polypyrrole Composite

0.34g of TiTe-nCeP$_f$ sheet was immersed in a mixture of 5ml of 4% aniline and 3.75 ml 4% pyrrole in ethanol, left at room temperature for 48h. The impregnated sheet was removed, washed with distilled water and ethanol and left to dry in air. The colour of the resultant product was blackish-green.

2.11. Ion Exchange Capacity

The ion exchange capacity of nanosized fibrous cerium(iv) phosphate, $Ce(HPO_4)_2.2.9H_2O$ was determined by addition of 25 ml of 0.1M NaCl solution to 100 mg of nCeP$_f$, with stirring for one hour, then titrated with 0.1 M NaOH solution.

2.12. Estimation of Water of Hydration of (TiTe-nCeP$_f$) and (ZrTe-nCeP$_f$) Nano Composite Membranes

100mg of (TiTe-nCeP$_f$), or (ZrTe-nCeP$_f$), was heated at 150°C for 1 hour. The % weight loss was calculated, which is

related to the loss of water of hydration, found to be 8.81% and 10.0 %, respectively.

2.13. Separation of Polymers from Composites via HF Solution

To 0.1g of TiTe-, ZrTe- nCeP$_f$ / conductive polymer nanocomposite membrane in plastic container, 10 ml of 6M HF solution was added, subjected to stirring for 24h. The remaining material, the polymer, was collected by filtration, washed with distilled water, acetone and ethanol and allowed to dry in air.

3. Results and Discussion

Nanofibrous cerium phosphate membrane, $Ce(HPO_4)_2.2.9H_2O$ (nCeP$_f$), was prepared and characterized by chemical, XRD, TGA, FT-IR and SEM.

3.1. XRD

XRD of (nCeP$_f$) is shown in Figure 1, with d_{001} = 10.89Å.

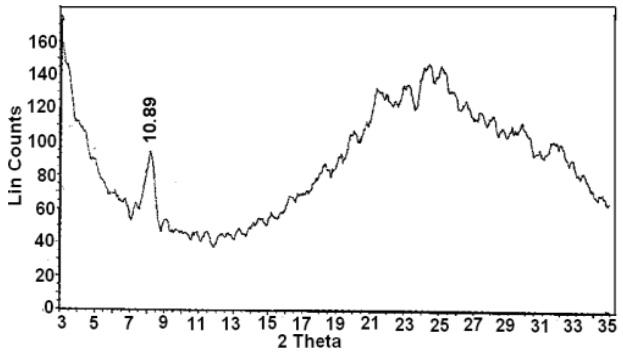

Figure 1. XRD of (nCeP$_f$)

3.2. TGA

Thermogram of (nCeP$_f$) is shown in Figure 2. The thermal decomposition occurs in continuous process, The thermal analysis was carried out at temperatures between 10-775°C, the final product was CeP_2O_7. Loss of water of hydration occurs between 60-200°C, followed by POH groups condensation. The total weight loss found to be equal to 19.09%.

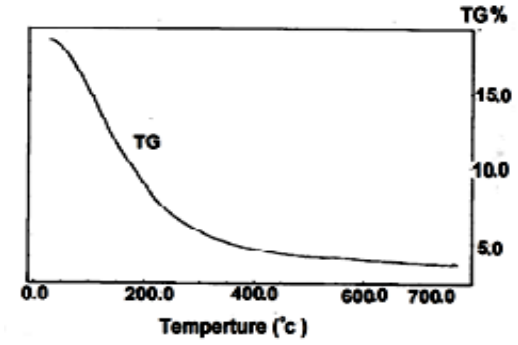

Figure 2. TGA of (nCeP$_f$)

3.3. FT-IR

Figure 3 shows FT-IR spectrum of fibrous $Ce(HPO_4)_2.2.9H_2O$, with a trend similar to that of M(IV) phosphates. It consists of broad band centered at 3350cm^{-1} is due to OH groups symmetric stretching of H_2O, small sharp band at 1628cm^{-1} is related to H-O-H bending, and sharp broad band centered at 1045cm^{-1} is corresponds to phosphate groups vibration The bands at the region 630-450 cm^{-1} are ascribe the presence of $\delta(PO_4)$.

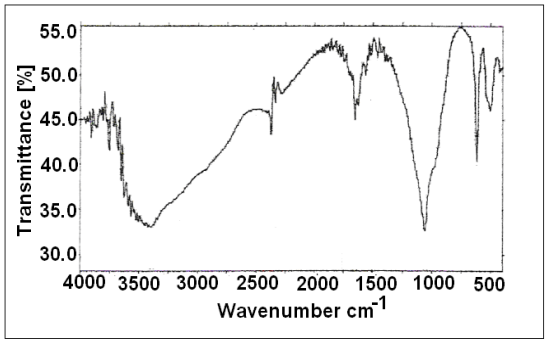

Figure 3. FT-IR of (nCeP$_f$)

3.4. SEM

SEM morphology image of the nanosized fibrous cerium phosphate (nCeP$_f$) is shown in Fig. 4. The photograph shows its average size is ~20.5 nm.

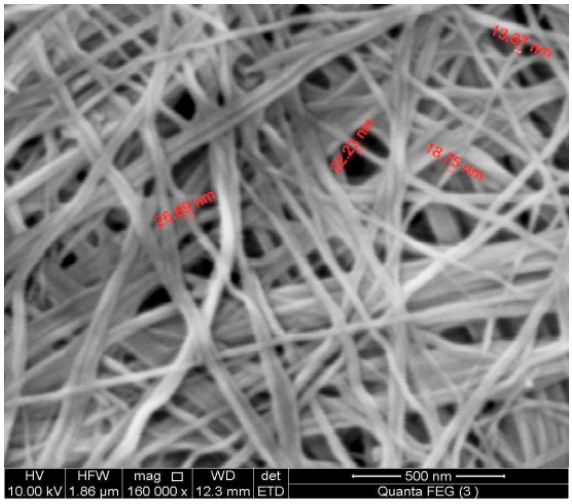

Figure 4. SEM morphology image of (nCeP$_f$)

Glassy titanium tellurate and zirconium tellurate, $TiO(HTeO_4)_2.3.99H_2O$, $ZrO(HTeO_4)_2.3.35H_2O$, respectively, were prepared and characterized, found to be similar to that reported by Shakshooki etal [63].

3.5. XRD of Glassy Titanium-, Zirconium Tellurates

Figure 5 shows typical XRD spectrum of the glassy ($M^{IV}Te$), shows amorphous trend, (M= Ti, Zr).

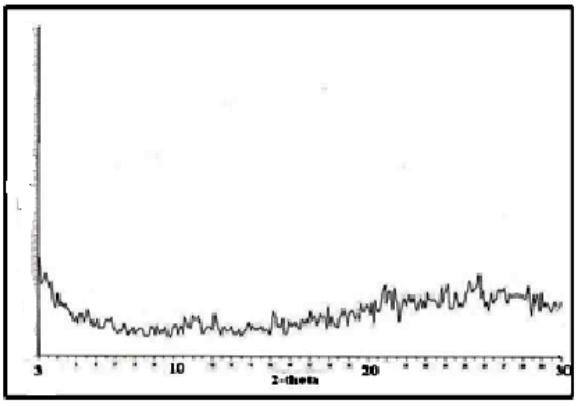

Figure 5. Typical XRD of glassy ($M^{IV}Te$)

3.6. FT-IR Spectrum of Glassy Zirconium-, Titanium Tellurates

Figure 6 shows FT-IR spectrum of glassy $ZrO(HTeO_4)_2.3.35H_2O$, represents typical FT-IR spectra of M^{iv} tellurates, exhibit broad band centered at 3300 cm^{-1} corresponds to OH-symmetric and asymmetric stretching. Medium band at1625 cm^{-1} attributed to H-O-H bending, Band at 750 cm^{-1} can be attributed to Te-OH, $HTeO_4$, band at 500 cm^{-1} is related to Te-O bond [63].

Figure 7 shows FT-IR spectra of $TiO(HTeO_4)_2.3.99H_2O$ found to follow similar FT-IR spectrum trend of glassy $M^{IV}Te$ [63].

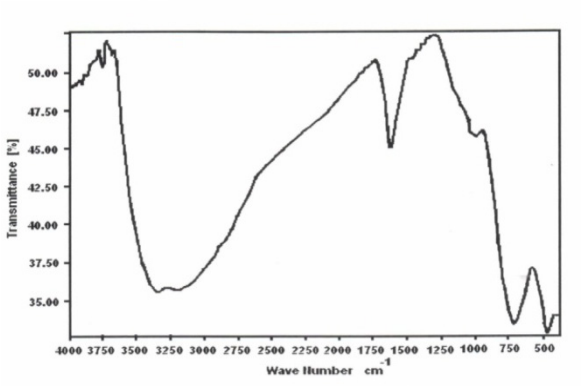

Figure 6. FT-IR of $ZrO(HTeO_4)_2.3.35H_2O$

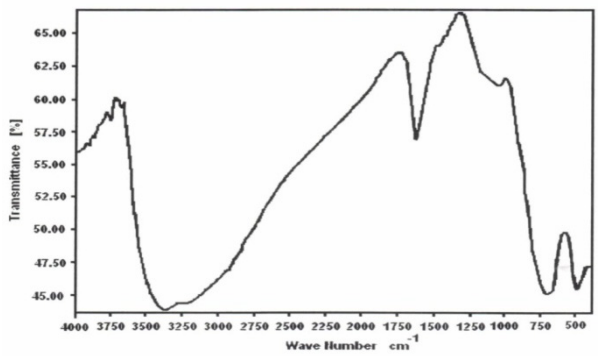

Figure 7. FT-IR of $TiO(HTeO_4)_2.3.99H_2O$

3.7. Thermal Behavior (TG/DTA) of the Glassy Zirconium-, Titanium Tellurates

Thermal analysis, TGA, is a good tool for characterization of tetravalent metal phosphates and tetravalent metal tellurates [63]. Figures (8,9) show the thermogram, TGA/DTA, of the resultant glassy zirconium-, titanium tellurates. TG/DTA of glassy zirconium tellurate is given in Figure 8, indicates endothermic process accompanied with weight loss. The final product was ZrO_2. Te_2O_6. The total weight loss found to be 19.96%, accordingly it was formulated as $ZrO(HTeO_4)_2.3.35H_2O$.

TG/DTA of glassy titanium tellurate is given in Figure 9, indicates endothermic process accompanied with weight loss. The final product was TiO_2. Te_2O_6. The total weight loss found to be 20.962%, accordingly it was formulated as $TiO(HTeO_4)_2.3.99H_2O$.

Schematic representation of thermal behavior of glassy M^{iv} Tellurates, where M=Zr,Ti.

$(M^{iv}O(HTeO_4)_2.nH_2O) - [(nH_2O)$

and–(structural water)] → $M^{iv}O_2$.+Te_2O_6.

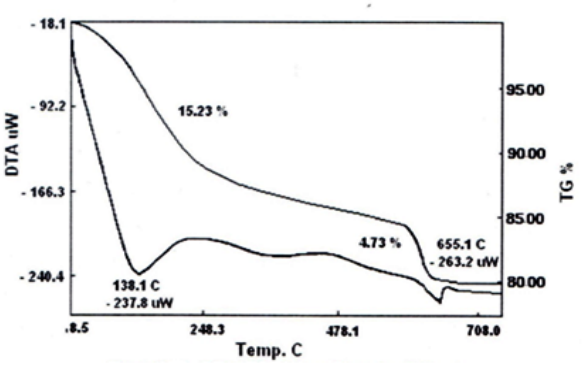

Figure 8. TG/DTA of glassy $ZrO(HTeO_4)_2.3.35\ H_2O$

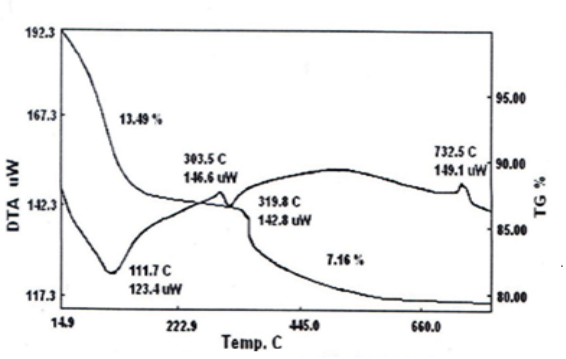

Figure 9. TG/DTA of glassy $TiO(HTeO_4)_2.3.99H_2O$

Novel glassy titanium-, zirconium tellurates - fibrous cerium phosphate nanocomposite membranes, $[TiO(HTeO_4)_2]_{0.25}$ $[Ce(HPO_4)_2]_{0.75}$. $1.75H_2O$ ($TiTe\text{-}nCeP_f$), $[ZrO(HTeO_4)_2]_{0.25}$ $[Ce(HPO_4)_2]_{0.75}.2.11H_2O$($ZrTe\text{-}nCeP_f$), respectively, were prepared and characterized.

3.8. (TiTe-nCeP$_f$)/ polyaniline-/ polyindole-/ polypyrrole Nanocomposite Membranes

On immersing of $[TiO(HTeO_4)]_{0.25}$ $[Ce(HPO_4)_2]_{0.75}.1.75H_2O$ nanocomposite membrane in ethanol solutions of aniline, indole, and pyrrole, respectively, the color of self supported sheet gradually changes with time to dark green, brown and black, respectively. A possible explanation is that polymerization of monomers were promoted by the reduction nCeP$_f$ present on the surface of the fiber cerium phosphate is attacked by monomers, converted to cerium (III) orthophosphate ($CePO_4$). Self-supported sheet integrity was preserved.

The resultant materials were characterized by elemental (C,H,N) analysis, FT-IR, and scanning electron microscopy (SEM). From elemental (C,H,N) analysis the amount of organic materials present in (TiTe-nCeP$_f$)/ polyaniline-, polyindole-, polypyrrole composites were (14.88, 11.87, 10.73 % in wt), respectively.

3.9. (ZrTe-nCeP$_f$)/ polyaniline-/ polyindole-/ polypyrrole Nanocomposite Membranes

On immersing of $[ZrO(HTeO_4)]_{0.25}$ $[Ce(HPO_4)_2]_{0.75}$. $1.75H_2O$ nanocomposite membrane in ethanol solutions of aniline, indole and pyrrole, respectively, the color of self supported sheet gradually changes with time to dark green, brown and black, respectively. A possible explanation is that polymerization of monomers were promoted by the reduction nCeP$_f$ present on the surface of the fiber cerium phosphate is attacked by the monomers, converted to cerium (III) orthophosphate ($CePO_4$). Self-supported sheet integrity was preserved.

The resultant materials were characterized by elemental (C,H,N) analysis, FT-IR, and scanning electron microscopy (SEM). From elemental (C,H,N) analysis the amount of organic materials present in (ZrTe-nCeP$_f$)/ polyaniline-, polyindole-, polypyrrole composites were (22.8, 5.52, 7.58% in wt), respectively.

3.10. SEM Morphology Images of (TiTe-nCeP$_f$) /polyaniline-/polyindole-/ polypyrrole\ nano Composite Membranes

SEM morphology images of the resultant (TiTe-nCeP$_f$)/ conductive polymers are shown in Figures (10-12), respectively, reveal a distribution of the polymer on the inorganic matrix (TiTe-nCeP$_f$).

3.11. SEM Morphology Images of (ZrTe-nCeP$_f$)/polyaniline-/polyindole-/ polypyrrole Nanocomposite Membranes

SEM morphology images of the resultant (ZrTe-nCeP$_f$)/ conductive polymers are shown in Figures (13-15), respectively, reveal a distribution of the polymer on the inorganic matrix (ZrTe-nCeP$_f$).

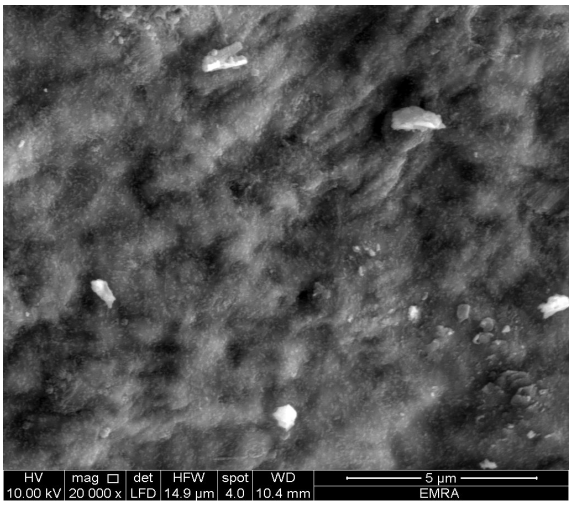

Figure 10. SEM morphology image of (TiTe-nCeP$_f$)/ polyaniline composite

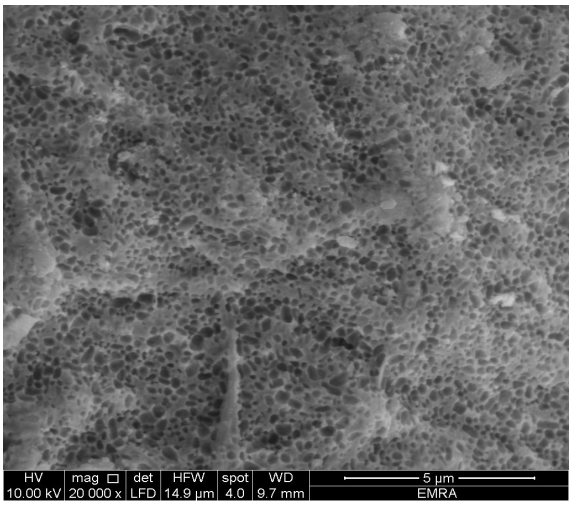

Figure 11. SEM morphology image of (TiTe-nCeP$_f$)/ polyindole composite

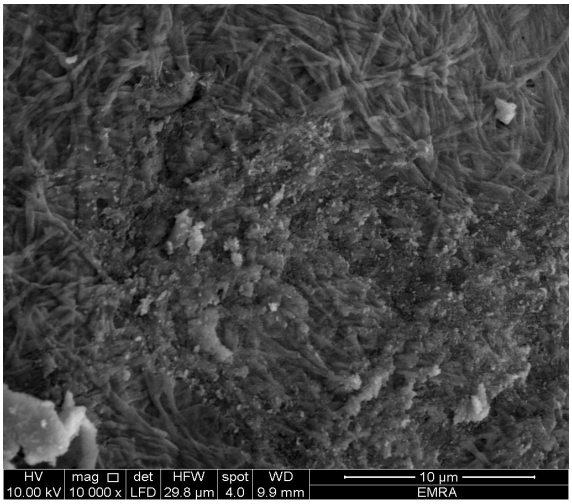

Figure 12. SEM morphology image of (TiTe-nCeP$_f$)/ polypyrrole composite

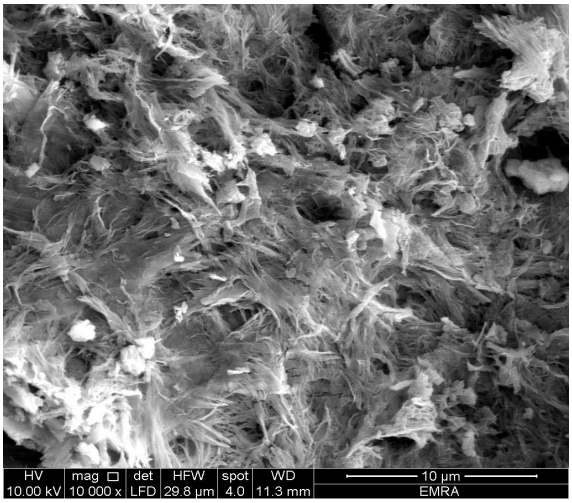

Figure 13. SEM morphology image of ($ZrTe\text{-}nCeP_f$)/ polyaniline composite

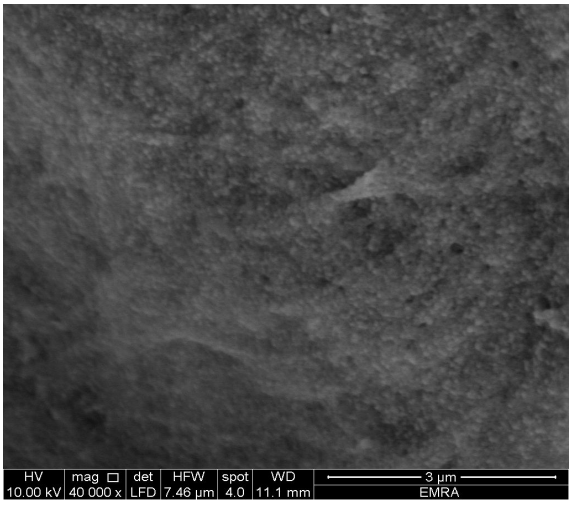

Figure 14. SEM morphology image of ($ZrTe\text{-}nCeP_f$)/ polyindole composite

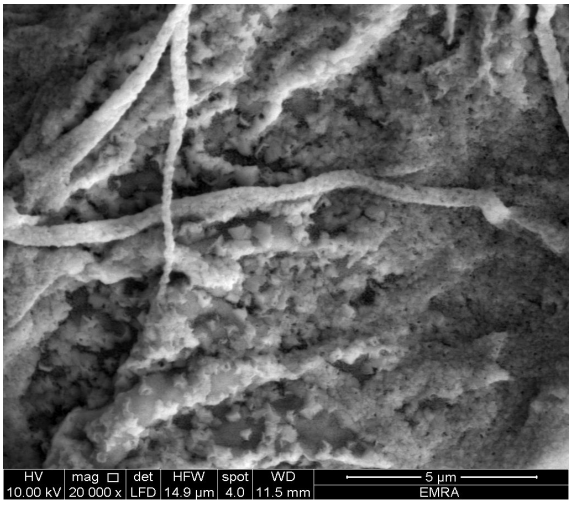

Figure 15. SEM morphology image of ($ZrTe\text{-}nCeP_f$)/ polypyrrole composite

3.12. FT-IR Spectra of Resultant Conductive Polymers Composites

FT-IR spectroscopy became a key tool to investigate structure of conductive polymers and their composites.

Figure 16(a,b,c) show FT-IR spectra of ($TiTe\text{-}nCeP_f$)/ polyaniline-, polyindole-, polypyrrole composites, respectively. Small sharp band at 1600 cm^{-1} is related to H-O-H bending, and broad band centered at 988- or at 1000 cm^{-1} is corresponds to phosphate groups vibration, small sharp at 750 cm^{-1} may attribute to $HTeO_4$, TiOH groups vibration. The band in the range 2000-1200 cm^{-1} corresponds to C-C bonds C-H (aromatic) stretching, C=C stretching. C-N stretching.

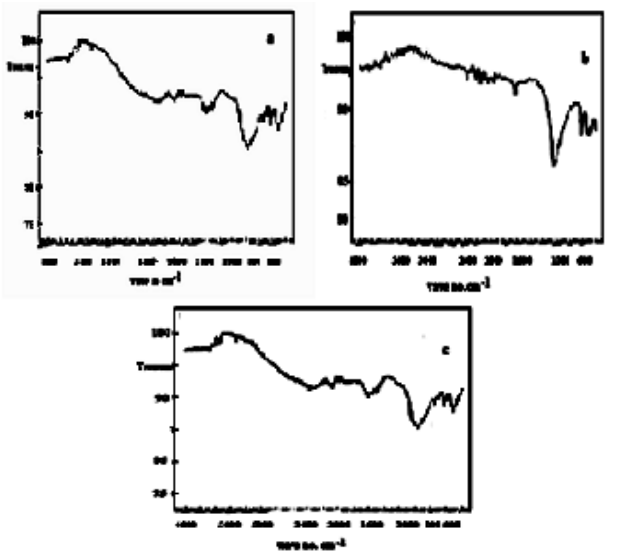

Figure 16(a,b,c). FT-IR spectra of ($TiTe\text{-}nCeP_f$)/ polyaniline-, polyindole-, polypyrrole composites, respectively

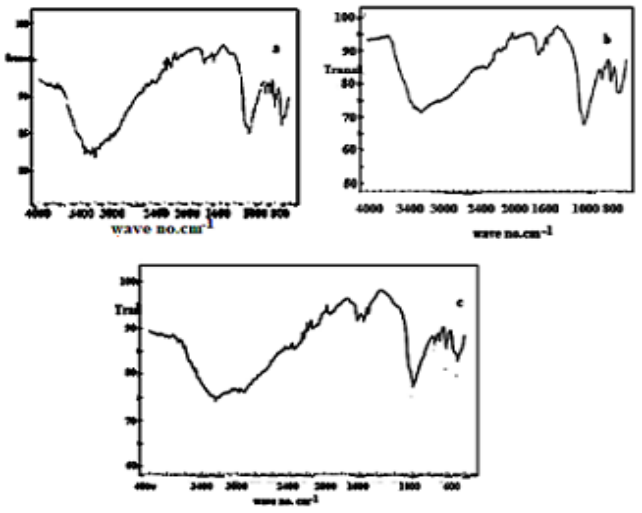

Figure 17(a,b,c). FT-IR spectra of ($ZrTe\text{-}nCeP_f$)/ polyaniline-,polyindole-, polypyrrole composites, respectively

Figure 17(a,b,c) show FT-IR spectra of ($ZrTe\text{-}nCeP_f$)/ polyaniline-, polyindole-, polpyrrole,- composites, respectively. The resultant FT-IR spectra follow almost same

trend. Intensity and shifting of certain bands may attributed to nature of the resultant conductive polymer. Bands, arise from broad band at 3342 cm^{-1}, is due to OH groups symmetric stretching of H_2O while the band at 3196 cm^{-1} is related to N–H stretching. Small sharp band at 1600 cm^{-1} is related to H-O-H bending, and broad band centered at 1000 cm^{-1} is corresponds to phosphate groups vibration, small sharp band at 750 cm^{-1} may attribute to $HTeO_4$, TiOH groups vibration. The bands in the range 2196 - 1200 cm^{-1} corresponds to C-H stretching, C-C bonds C-H (aromatic) stretching, C=C stretching, C-N stretching.

3.13. (TiTe-nCeP$_f$)/ polyaniline-copolyindole Composite

When TiTe-nCeP$_f$ sheet was immersed in solution of mixture of aniline: indole(1:1), the resultant product was (TiTe-nCePf)/ polyindole-co-polyaniline composite. It was characterized by elemental (C, H, N) analysis, SEM and FT-IR spectroscopy. From elementals (C, H, N) analysis. The amount of organic material found to be (Pani = 9.92, PIn = 10.43 % in wt). The color of the product was green.

3.13.1. SEM of (TiTe-nCeP$_f$)/ polyaniline-co -polyindole Composite

Figure (18) shows SEM image of (TiTe-nCeP$_f$) / polyaniline-co-polyindole composite, reveal a distribution of the copolymer on the inorganic matrix

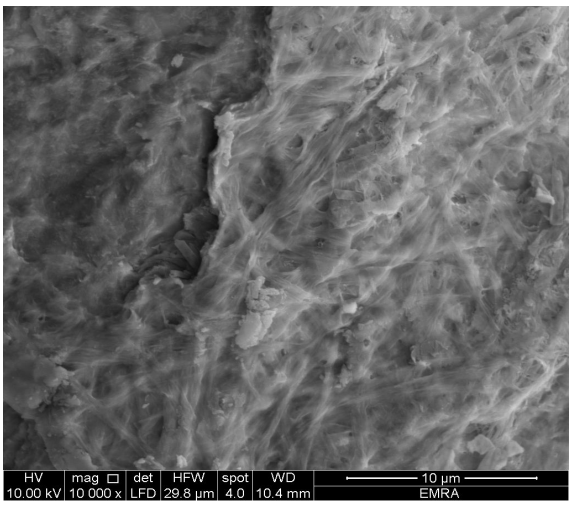

Figure 18. SEM image of (TiTe-nCePf)/ polyaniline-co-polyindole composite

3.13.2. FTIR of (TiTe-nCePf) / polyaniline-co-polyindole Composite

Figure (19) shows FT-IR spectrum (TiTe-nCePf) / polyaniline-co-polyindole composite. Band at at ~2375 cm^{-1} corresponds to C-H stretching, band at ~2924 cm^{-1} corresponds to C-H bonds, The presence of bands in the range of 2016- 1492 cm^{-1} correspond to stretching C-C bonds characteristic of indole unites, C-H (aromatic) stretching, C=C stretching (between two indole units) and depicts the presence of benzenoid rings also C=C stretching vibration of benzenoid ring. Broad (doublet) band at range 1061-970 cm^{-1} corresponds to phosphate groups vibration, band at 741 cm^{-1} may attribute to $HTeO_4$, TiOH groups vibration.

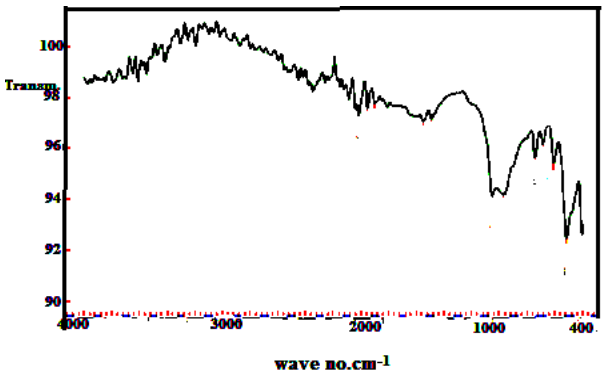

Figure 19. FT-IR spectrum (TiTe-nCePf) / polyaniline-co-polyindole composite

3.14. (TiTe-nCePf)/ polyaniline-co-polypyrrole Composite

When TiTe-nCeP$_f$ sheet was immersed in solution of mixture of aniline: polypyrrole(1:1), the resultant product was (TiTe-nCePf)/ polyaniline-co-polypyrrole composite. It was characterized by elemental (C, H, N) analysis, SEM and FT-IR spectroscopy. From elemental (C, H, N) analysis. The amount of organic materials found to be (Pani = 16.24, PPy = 4.68 % in wt). The color of the product wasblackish green.

3.14.1. SEM of (TiTe-nCePf)/polyaniline-co -polypyrrole Composite

Figure (20) shows SEM image of (TiTe-nCePf) / polyaniline-co-polypyrrole composite, reveal a distribution of the copolymer on the inorganic matrix.

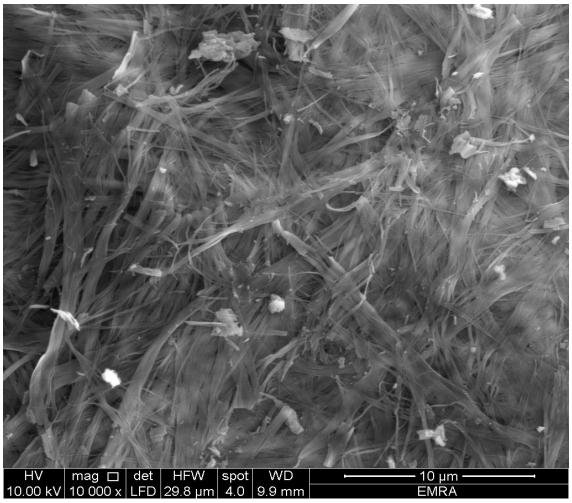

Figure 20. SEM image of (TiTe-nCePf)/ polyaniline-co-polypyrrole composite

3.14.2. FTIR of (TiTe-nCePf) / polyaniline-co-polypyrrole Composite

Figure (21) shows FT-IR spectrum (TiTe-nCePf) / polyaniline-co-polypyrrole composite. The spectrum shows broad band in the range 3675-2400 cm^{-1} centered at 3025

cm^{-1} can be considered for OH groups symmetric stretching of H_2O and also related to N–H stretching. Bands at 2375 and at 2121 cm^{-1} corresponds to C-H stretching., The presence of bands in the range of 1800- 1494 cm^{-1} correspond to stretching C-C bonds characteristic of indole unites, C-H (aromatic) stretching, C=C stretching (between two indole units) and depicts the presence of benzenoid rings also C=C stretching vibration of benzenoid ring. Broad centered at 995 cm^{-1} corresponds to phosphate groups vibration, band at 751 cm^{-1} may attribute to $HTeO_4$, Ti-OH groups vibration.

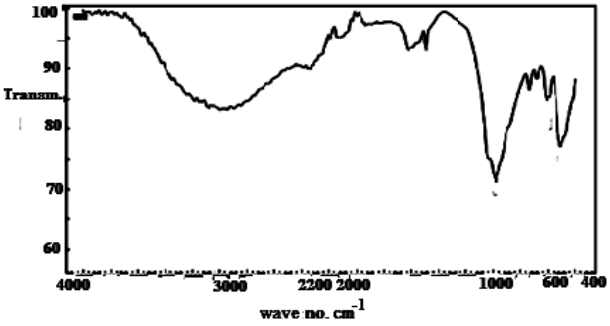

Figure 21. FTIR spectrum of (TiTe-nCePf) / polyaniline-co-polypyrrole composite

3.15. (ZrTe-nCePf)/polyaniline-co-polyindole Composite

When ZrTe-nCeP_f sheet was immersed in solution of mixture of aniline: polypyrrole(1:1), the resultant product was (TiTe-nCePf)/ polyaniline-co-polypyrrole composite. It was characterized by elemental (C, H, N) analysis, SEM and FT-IR spectroscopy. From elemental (C, H, N) analysis. The amount of organic material found to be (Pani = 9.55, PPy = 5.1% in wt). The color of the product was blackish green.

3.15.1. SEM of (ZrTe-nCePf)/polyaniline -co-polyindole Composite

Figure (22) shows SEM image of (TiTe-nCePf) / polyaniline-co-polyindole composite, reveal a distribution of the copolymer on the inorganic matrix.

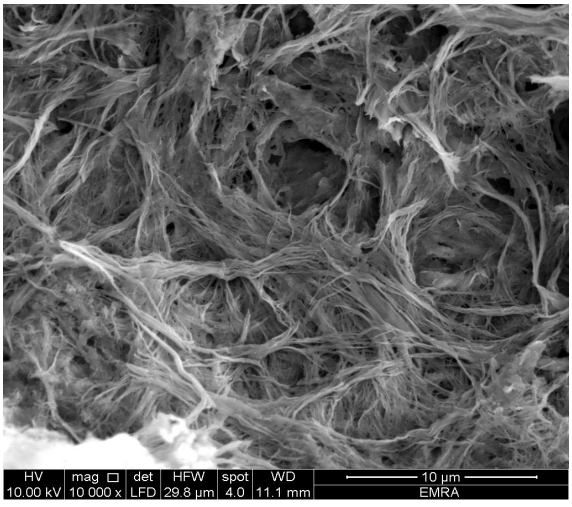

Figure 22. SEM image of (ZrTe-nCePf)/ polyaniline-co-polyindole composite

3.15.2. FT-IR Spectrum of (ZrTe-nCePf) / polyaniline-co-polyindole Composite

Figure (23) shows FT-IR spectrum (ZrTe-nCePf) / polyaniline-co-polyindole composite. Band at 2335 cm^{-1} corresponds to C-H stretching., The presence of bands in the range of 2016-1300 cm^{-1} correspond to stretching C-C bonds characteristic of indole unites, C-H (aromatic) stretching, C=C stretching (between two indole units) and depicts the presence of benzenoid rings also C=C stretching vibration of benzenoid ring. Broad centered at 995 cm^{-1} corresponds to phosphate groups vibration, band at 751 cm^{-1} may attribute to $HTeO_4$, Zr-OH groups vibration.

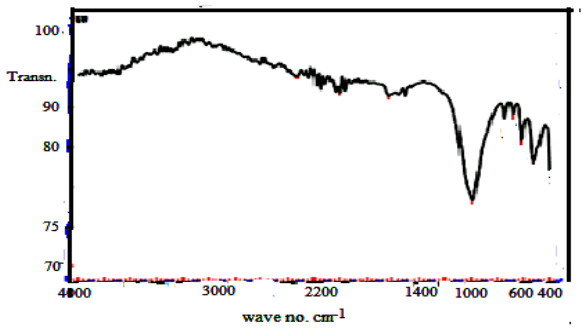

Figure 23. FTIR of (ZrTe-nCePf) / polyaniline-co-polyindole composite

3.16. (ZrTe-nCePf)/polyaniline-co-polypyrrole Composite

When ZrTe-nCeP_f sheet was immersed in solution of mixture of aniline: polypyrrole(1:1), the resultant product was (TiTe-nCePf)/ polyaniline-co-polypyrrole composite. It was characterized by elemental (C, H, N) analysis, SEM and FT-IR spectroscopy. From elemental (C, H, N) analysis. The amount of organic materials found to be polypyrrole (Pani = 16.24, PPy = 4.68 % in wt). The color of the product was blackish green.

3.16.1. SEM of (ZrTe-nCePf)/ polyaniline -co-polypyrrole Composite

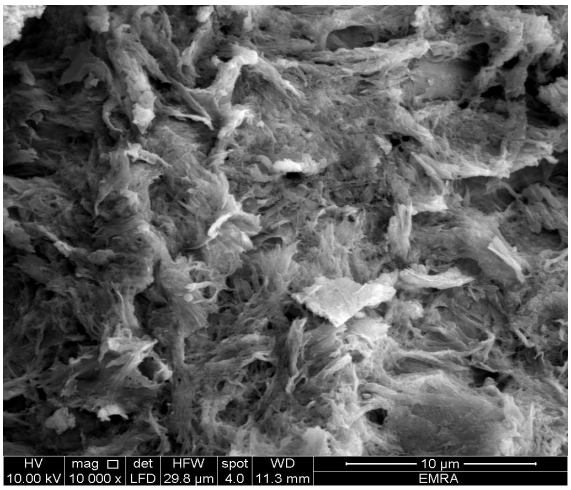

Figure 24. SEM image of (ZrTe-nCePf)/ polyaniline-co-polypyrrole composite

Figure (24) shows SEM image of (TiTe-nCePf)/polyaniline-co-polypyrrole com -posite, reveal a distribution of the copolymer on the inorganic matrix.

3.16.2. FT-IR Spectrum of (ZrTe-nCePf) / polyaniline-co-polypyrrole Composite

Figure (25) shows FT-IR spectrum (ZrTe-nCePf) / polyaniline-co-polyindole composite. Bands at ~ 2349, 2120 cm^{-1} corresponds to C-H stretching., The presence of bands in the range of 2000-1404 cm^{-1} correspond to stretching C-C bonds characteristic of indole unites, C-H (aromatic) stretching, C=C stretching (between two indole units) and depicts the presence of benzenoid rings also C=C stretching vibration of benzenoid ring. Broad centered at 984 cm^{-1} corresponds to phosphate groups vibration, band at 740 cm^{-1} may attribute to $HTeO_4$, Zr-OH groups vibration.

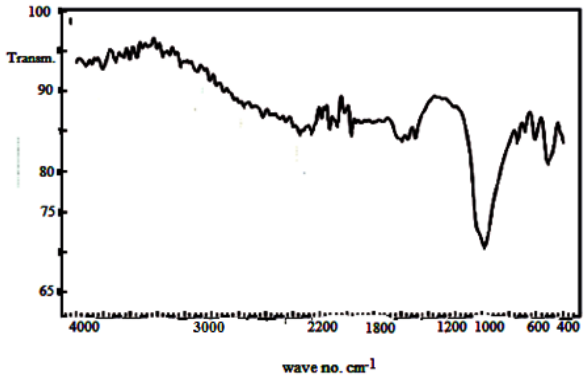

Figure 25. FT-IR spectrum of (ZrTe-nCePf) / polyaniline-co-polypyrrole composite

4. Conclusions

Glassy titanium tellurate, $TiO(HTeO_4)_2$. 3.99 H_2O (TiTe), Glassy zirconium tellurate, $ZrO(HTeO_4)_2$. 3.35H_2O (ZrTe), nanofibrous cerium phosphate, $Ce(HPO_4)_2$. 2.9H_2O ($nCeP_f$) and Their novel nanocomposite membranes $[TiO(HTeO_4)_2]_{0.25}$ $[Ce(HPO_4)_2]_{0.75}$. 1.75H_2O (TiTe-$nCeP_f$), $[ZrO(HTeO_4)_2]_{0.25}$ $[Ce(HPO_4)_2]_{0.75}$. 2.11H_2O (ZrTe-$nCeP_f$), respectively, were prepared and characterized.

Their /polyaniline-, polyindole-, polypyrrole-, polyaniline–co-polyindole-, polyaniline-co- polypyrrole nanocomposite membranes were prepared via in-situ chemical oxidation of the monomers aniline, indole, pyrrole and their co-monomers, that was promoted by the reduction of Ce(iv) ions present in the inorganic matrix. The presence of Ce(iv) ions allows redox reactions necessary to oxidative polymerization to occur. A possible explanation is that polymerization of the copolymerization of the co-monomers were promoted by the reduction of some of $nCeP_f$ present in composite, that attacked by monomers, and the co-monomers, respectively, converted to cerium(III) orthophosphate ($CePO_4$).

The formulation of the resultant conductive nanocomposites was supported by elemental(C,H,N) analysis, FT-IR spectra and SEM. Color changes supports the formation of the resultant organic polymers composites. We suggest self doping occurred on polymerization, which is due to H^+ present in (=TeOH) groups.

The % in wt of polymer found to be in agreement with the % in wt contents of that recovered from selected testing experiments using HF solution. Beneficial properties of the resultant nanocomposites can be considered these composites as novel conducting inorganic-organic composites, ion exchangers, solid acid catalyst and as sensors.

ACKNOWLEDGEMENTS

To Department of Chemistry, Faculty of Science, University of Tripoli . Tripoli, Libya and Department of Chemistry, Faculty of Science, University of Sebha. Sebha, Libya for supporting of this research.

REFERENCES

[1] Street, G. B., Clarke, T. C., Conducting Polymers: A Review of Recent Work IBM J. Res. Dev. 25(1981) pp51–57.

[2] T. J. Skotheim, J. R. Reynolds, Eds. Handbook of Conducting Polymers, Third Ed., CRC Press, Boca Raton, USA (1997).

[3] H. S. Nalwa, Ed. Handbook of Organic Conductive Molecules and Polymers, Vol. 2, John Wiley, Chichester, UK (1997).

[4] MacDiarmid, A. G., A novel role for organic polymers, Angewandte Chemie International Edition, 40 (2001)2581.

[5] Heeger, A., Semiconducting and metallic polymers: The fourth generation of polymeric materials, Reviews of Modern Phys, 73(2001)681.

[6] Freund, M.S. and Deore, B.A. Edts., Self Doped Conducting Polymers, John Wiley and Sons (2007).

[7] Lange, U., Roznyatovskaya, N. V., Mirsky, Vladimir M., Conducting polymers in chemical sensors and arrays, Analytica Chimica Acta vol. 614 issue (2008).

[8] Kucheldorf, H.R., Luken, O. and Swift, G., Hand book of polymer synthesis, 2nd Edit., CRC Press (2010).

[9] Banerjee, S. and Tayagi, A.K. Edts, Functional Materials: Preparation, Proscessing and Applications, Elsevier (2012).

[10] Lange, U., Roznyatovskaya, N. V., Mirsky, Vladimir M., Conducting polymers in chemical sensors and arrays, Analytica Chimica Acta vol. 614 issue (2008).

[11] Sapurina, I. Y. and Shishov, M. A., New polymers for special applications, Ailton De Souza Gomes, Ed. (2012).

[12] Cai, Z., Grang, M. and Tang, Z., Novel battery using

conducting polymers: and polyaniline, J. of Mater. Sci., 39(2004) 4001.

[13] Ćirić-Marjanović, G., Polyaniline nanostructures, in nanostructured conductive polymers, (Eftekhari, A. ed., John Wiley & Sons, Ltd(2010).

[14] Vernitskaya, T.V. Tat'yana, V.V. and Efimov, Polypyrrole: a conducting polymer; its synthesis, properties and applications, Russ. Chem. Rev., (1997) pp66 443.

[15] Feng-Hao Hsu, F.H and, Wu, T.M., In situ synthesis and characterization of conductive polypyrrole/graphene composites with improved solubility and conductivity, Synthetic Metals, 162(2012) pp682–687.

[16] Fajan, A. and Been, B., structural and optical properties of polyindole manganese oxide nanocomposite, Indian J. of Adv. in Chem. Sci., 2 (2013) pp95-96.

[17] Wang, C. Yu, Hao, C., Chen,K., Clip-like polyaniline nanofiber synthesized by an in-situ chemical oxidative polymerization and its strong electro rheological behavior, 239(2018) pp1-12.

[18] A.G. Green, A.E. Woodhead, J. Chem. Soc., 1910 (1997) pp2388−2403.

[19] A. K. Sharma, Y. Sharma, *J*. Electrochem. Sci. Eng. 3 (2013) pp47–56.

[20] M. Magioli, B. G. Soares, A. S. Sirqueira, M. Rahaman, D. Khastgir, J. Appl. Polym. Sci., 125 (2012) pp1476–1485.

[21] M. Rahaman, L. Nayak, T. K. Chaki, D. Khastgir, Adv. Sci. Lett., 18 (2012) pp54−61.

[22] S. Bhadra, D. Khastgir, Polym. Test., 27 (2008) pp 851–857.

[23] S. Bhadra, S. Chattopadhyay, N.K. Singha, D. Khastgir, J. Appl. Polym. Sci., 108 (2008) pp57–64.

[24] M. Rahaman, T. K. Chaki, D. Khastgir, J. Appl. Polym. Sci., 128 (2013) pp161−168.

[25] S. Bhadra, D. Khastgir, N.K. Singha, J.H. Lee, Prog. Polym. Sci., 34 (2009) pp783–810.

[26] J.C. Chiang, A.G. MacDiarmid, Synth. Met., 13 (1986) pp193–205.

[27] W. Hualan, H. Qingli, Y. Xujie, L. Lude, W. Xin, Electrochem. Commun., 11 (2009) pp1158–1161.

[28] J.P. Zheng, P.J. Cygan, T.R. Jow, J. Electrochem. Soc., 142 (1995) 2699.

[29] A.J. Burke, J. Power Sources*,* 91 (2000) 37.

[30] B.E. Conway, Electrochemical Super capacitors, Kluwer-Plenum, New York (1999).

[31] S. Sopčić, M. Kraljić Roković, Z Mandić, J. Electrochem. Sci. Eng. 2 (2012)pp 41–52.

[32] S. Chandra, et al., Chem. Phys. Lett*.,* pp519–520 (2012) 59–63.

[33] Sh. M. Ebrahim, Sh. M., Abd-ElLatif, M.M., Gad, A.M. and Soliman, M.M., Cyclic voltammetry and impedance studies of electrodeposited polypyrrole nanoparticles doped with 2-acrylamido-2-methyl-1-propanesulfonic acid sodium salt, Thin Solid Films, 518(2010) pp4100-4105.

[34] Lee, J.K., Jeong, H., Lassarote, R., Lavall, R.L., A, Busnaina, A., Younglae Kim, Y., Jung, Y.J., and Lee, H.Y., Polypyrrole films with micro/nanosphere shapes for electrodes of high-performance supercapacitors, *ACS Appl. Mater. Interfaces,* 9 (2017) pp33203–33211.

[35] Chitte, H.K., Shinde, G.N., Bhat, N.V. and Walunj, V.E., Synthesis of Polypyrrole Using Ferric Chloride ($FeCl_3$) as Oxidant Together with Some Dopants for Use in Gas Sensors, Journal of Sensor Tech., 1(2011) pp2161-1238.

[36] Hai; V.V.T., Hang, To Thi Xuan, H.T.T, Thi, N., P, Thom, N.T. Nguyen Thi, N. Didier, D.,T., Thi Mai, D.T., Synthesis of silica/polypyrrole nanocomposites and application in corrosion protection of carbon steel, J.of NanoSc. and Nanotech., 18(2018) pp. 4189-41957.

[37] Ermişn, N. and Tınkılıç, N., Preparation of molecularly imprinted polypyrrole modified gold electrode for determination of tyrosine in biological samples Int. J. Electrochem. Sci., 13 (2018) pp2286-2298.

[38] Billand, B.; Maarouf, E.; Hamecant, E. An Investigation of Electrochemically and Chemically Polymerized Polyindole. Mater. Rech. Bull. 29(1994) 1239.

[39] Fajan, A.; Been, B. Structural and Optical Properties of Polyindole manganese Oxide Nanocomposite. Indian J. ofAdv. In Chem. Sci., 2(2013) pp95-96.

[40] Kucheldorf, H. R.; Luken, O.; Swift, G. Handbook of Polymer Synthesis; CRC Press (2010).

[41] Cai, Z.; Grang, M.; Tang, Z. Novel Battery Using Conducting Polymers and Polyaniline. J. of Mater. Sci., 39(2004) pp 4001-400.

[42] Zhijiang, C.; Guang, Y. Synthesis Polyindole and Its Evaluation for Li-ion Battery Applications. Synth. Met. 160(2010) pp1902-1905.

[43] Dosio, S. T.; Mert, B. D.; Yazicch, B. Polyidole Top Coaton TiO2 for Corrosion Protection of Steel. Corrosion Sci. 66(2013) pp51-58.

[44] Rejani, P.; Beena, B. Structural and Optical Properties of Polyindole-Manganese Oxide Nanocomposite. Ind. J. of Adv. Chem. Sci. 2, (2013) pp95-99.

[45] Clearfield, A. Inorganic Ion Exchange Materials; CRCPress Fl.: Bocca Raton (1988).

[46] Colon, J. L.; Diaz, A.; Clearfeild, A. Nano encapsulation of Insulin into Zirconium Phosphate for Oral Delivery Applications, Biomacro Molecules, 9(2010)pp2465.

[47] Diaz, A.; Saxena, V.; Gunzalez, J.; David, A.; Casanas,B.; Carpenter, C.; et al. Zirconium Phosphate Nano-Platelets: A Novel Platform for Drug Delivery in Cancer Therapy. Chem. Commun., 48(2012) 1754.

[48] Tushato, M.; Danjo, M.; Baba, Y.; Murakom, M.; Nana, H. Preparation and Chemical Properties of a Novel Layered Cerium(IV) Phosphate. Bulletin of Chem. Soc. Jap., 70(1997) 143.

[49] Salvado, M. A.; Pertierra, P.; Tropajo, C.; Garcia, G. R., Crystal Structure of Cerium (IV) Bis (Hydrogen Phosphate Derivative. J. Am. Chem. Soc. 2007, 129(2007)10970.

[50] Alberti, G.; Costantino, U. Recent Progress in the Field of Synthetic Inorganic Exchanger Having a Layered and Fibrous Structure. J. Chromatogr., 102(1974) 5.

[51] Parangi, T.; Wani, P.; Chudasama, U. Synthesis, Characterization and Application of Cerium Phosphate, Desalination and Water Treatment, 38(2012)126.

[52] Romano, R.; Alves, O. S. Fibrous Cerium(IV) Phosphate Host of Weak and Strong Lewis Bases. Inclus. Phenom. and Macrocyclic, 51(2005) 211.

[53] Casciola, M.; Costantino, U.; Damico, S. Conductivity of Cerium(IV) Phosphate in Hydrogen Form. Solid StateIonics, 28(1988) 617.

[54] Varsheny, K. G.., Tayal, N.; Gupta, P.; Agrawal, A., Drabik, M. Synthesis, Ion-Exchange and Physical Studies on Polystyrene Cerium(IV) Phosphate Hybrid Fibrous Ion Exchanger. Ind. J. of Chem., 43(2004)2586.

[55] Metwally, S. S.; El-Gammal, B.; Ali, H. F.; Abo-EL-Enein, S. A. Removal and Separation of Some Radionuclides by Poly-Acrylamide Based Ce(IV)Phosphate. Separation Sci. and Tech., 46(2011)11.

[56] Alberti, G.; Casciola, M.; Captani, D.; Donnadio, A.; Narducci, R.; Pica, M.; et al. Novel Nafion-Zirconium Phosphate Composite Membranes with Enhanced Stability of Proton Conductivity, Electrochemica Acta, 52(2007) 8125.

[57] Yang, Y.; Liu, C.; Wen, H. Preparation and Properties of Polyvinyl Alcohol/Exfoliated α-Zirconium Phosphate, Polym. Test., 282(2009)185.

[58] Nagarale, R. K.; Shin, W.; Singh, P. K. Progress in IonicOrganic-Inorganic Composite Membranes for Fuel Cell Application. Polym. Chem., 1(2010) 388.

[59] Shakshooki, S. K.; Elejmi, A. A.; Khalfulla, A. M. and Elfituri, S. S, Polyvinylalcohol/ titanium phosphate nanocomposite membranes., Int. Conf. on Mater. Imperative, 11(2010) pp49-70.

[60] Shakchooki, S. K.; El-Akari, F. A.; El-Fituri, M. S. and El-Fituri, S. S. Fibrous Cerium(IV) Hydrogen Phosphate Membrane Self Supported Benzimidazole Polymerization, Agent. Adv. Mater. Res., 856, (2014)3.

[61] Sadek Khalifa Shakshooki, Nano Fibrous Cerium(IV) Hydrogen Phosphate Membrane Self Supported Indole Polymerization Agent,, J. Chem. Chem. Eng. 8 (2014) pp378-384.

[62] Shakshooki, S. K., El-Akari, F. A., Jangher, A. A. and Hamasi, A.M., Facile Synthesis of γ-Zirconium Phosphate-Fibrous Cerium Phosphate / Emeraldine Salt Nanocomposite Membrane, American Journal of Chemistry, 5 (2015) pp75-85.

[63] Shakshooki, S.K, El-Akari, F.A., El-Hamroni, S.M, Idris, R.H. and Aouzi, A.M., Synthesis and Characterization of Novel Highly Crystalline Layered Nanosized Zirconium-, Hafnium-, Titanium Tellurates from Their Parent Glassy Sodium Forms via HF Solution, J. of. Pharm. and Appl. Chem., 2(2016) pp205-210.